Proceedings of the Fortieth Turbomachinery Symposium
September 12-15, 2011, Houston, Texas

STABILITY CONSIDERATIONS – A SIMPLIFIED APPROACH

Urs Baumann
Head of Calculation and Development
MAN Diesel & Turbo Schweiz AG
CH-8005 Zurich, Switzerland
urs.baumann@man.eu

Urs Baumann is the Manager of the Calculation and Development department of MAN Diesel & Turbo Schweiz AG in Zurich, Switzerland. His responsibilities include the aerodynamic as well as the mechanical development and improvement of turbocompressors and associated components, as well as the implementation and maintenance of test stands and analytical tools needed to fulfill this task. His department comprises also a Product Development Group mainly focussing on high-speed motor driven, magnetically suspended compressors. He is the owner of several patents related to high pressure compression and high-speed oil-free motor compressors.

Before joining MAN Diesel & Turbo in 1996, Mr. Baumann worked for Sulzer Innotec, the Corporate Research and Development Center. For several years he was in charge of the machinery dynamics group which is responsible for the development, design improvement and trouble shooting on a wide range of Sulzer products.
Urs Baumann has a diploma (Mechanical Engineering, 1987) from the Swiss Federal Institute of Technology in Zurich.

ABSTRACT

In many cases it is necessary to judge the stability behavior of a specific compressor. This might be the OEM checking the feasibility of a proposed compressor layout or it might be the user judging one of his machines which causes troubles in operation. API 617 suggests a stability level I or level II analysis. The shortcoming of the level I analysis is that it considers only the global cross-coupling stiffness of the entire stages neglecting the actual seal design of a compressor. Thus the damping of a machine is always decreasing with increasing load which is not reflecting the true stability behavior of modern turbo compressors. On the other hand a level II analysis requires detailed insight into the machine design which might not be defined at that time or which is not known to the user.

To overcome these problems this tutorial proposes a different kind of stability check which only requires a minimum of operational and design data and delivers a comprehensible and (relatively) reliable picture of the stability behavior of the investigated compressor.

This tutorial derives the used stability criterion and explains the effect of the circumferential speed of the gas in the seal gap on the rotordynamic behavior. Finally it presents example calculations for different seal configurations and compares the resulting stability judgments to the results of the classical API level II analysis and to the results of experimentally determined rotor damping.

INTRODUCTION

There exists a long list of good and comprehensive lectures and courses about rotordynamic stability. These traditional approaches mainly deal with the “natural” physical requirement for a stable rotor, which is a positive modal damping (logarithmmic decrement) for the lowest whirling modes. In order to assess a rotor in this way, it is necessary to know all the design and operational details of the compressor and in addition all the required analytical tools such as bearing codes, seal codes and rotordynamics codes must be available. Correctly done this leads to a realistic statement about the stability of the machine for the operating condition taken into account.

Considering the difficulties and sometimes the impossibility to gather all the necessary information for a “real” stability calculation, this tutorial proposes a simplified approach which only needs data that is readily available. The proposed approach does not try to determine the “exact” damping of the rotor, it rather classifies the configuration to be stabilizing or destabilizing. This leads to the used stability criterion: A seal or an averaged combination of seals have to have a stabilizing effect on the rotordynamic behavior of the machine. Of course, this approach cannot, and does not try to,

substitute for a thorough analytical layout, but it gives a quick answer whether a specific configuration "works" or if the intended design will have to be improved. The proposed method also facilitates the insight into the influences of the different seal designs and swirl reducing features on the stability of the rotor.

This simplified approach mainly relies on the direct relationship between the so called "whirl frequency ratio" and the circumferential speed of the fluid within the seal gap. There is a more or less linear proportionality between relative circumferential speed and whirl frequency ratio. The simplification just substitutes the circumferential speed of the gas for the physically correct force ratio. This results in a very comprehensive representation of the stability criterion.

With the above assumptions it is possible to judge a given compressor design by simply knowing the circumferential speeds of the fluid in the seal gaps. Each labyrinth or seal type shows a characteristic circumferential speed as a function of the geometry (type), the seal length and the inlet swirl. Since this method does not consider the absolute level of the seal forces, it is necessary to weight the effects of the different seal gaps within the same machine. This can be done in different ways and levels of complexity. As a minimum the pressure differences over the seals have to be considered.

STABILITY CRITERION

The stability of a rotor is mainly influenced by the seal forces. The tangential seal forces determine the effective damping of the rotor whereas the radial seal forces have an impact on the stiffness of the rotor which also appears in the stability criterion (as the Flexi Ratio). The tangential seal forces can be written as:

$$F_\Theta = r_0 \cdot (K_{XY} - C_{XX} \cdot \omega) \tag{1}$$

where r_0 is the radius of the circular, synchronous orbit and ω is the precessional speed of the shaft. C_{XX} and K_{XY} are the direct damping and the cross-coupling stiffness coefficients, respectively. Equation (1) can be rewritten as follows:

$$F_\Theta = -C_{XX} \cdot r_0 \cdot \omega \cdot \left(1 - \frac{K_{XY}}{C_{XX} \cdot \omega}\right) = -C_{eff} \cdot r_0 \cdot \omega \tag{2}$$

where C_{eff} is the equivalent effective damping coefficient of the labyrinth seal. This leads to the following definition of C_{eff}:

$$C_{eff} = C_{XX} \cdot \left(1 - \frac{K_{XY}}{C_{XX} \cdot \omega}\right) \tag{3}$$

To ensure a stabilizing effect of the labyrinth, the effective damping must be positive which leads to the physically correct definition of the stability criterion and to the definition of the whirl frequency ratio based on the lowest whirling frequency (WFR_ω):

$$WFR_\omega = \frac{K_{XY}}{C_{XX} \cdot \omega} \quad < \quad 1 \tag{4}$$

Expanding Equation (4) by the rotational speed (Ω) of the shaft leads to:

$$WFR_\omega = \frac{K_{XY}}{C_{XX} \cdot \Omega} \cdot \frac{\Omega}{\omega} \quad = \quad WFR_\Omega \cdot FR \quad < \quad 1 \tag{5}$$

Where WFR_Ω is the whirl frequency ratio based on the rotational speed of the shaft and FR is the flexi ratio, which is a measure of the flexibility of the shaft at the speed of operation. Figure 1 visualizes the stability criterion given in Equation (5).

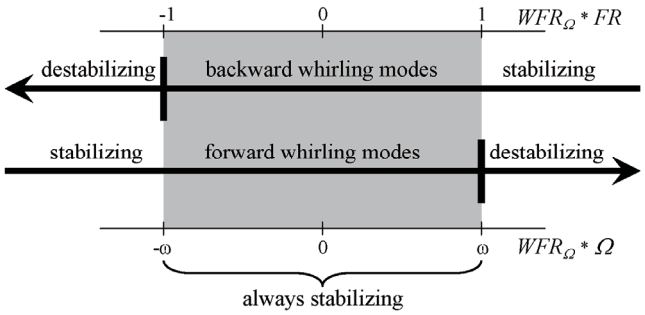

Figure 1. Visualization of the Stability Criterion.

ANALOGY AND SIMPLIFICATION

For the simplification we leave the physical part of Equation (5) (the part with C_{XX} and K_{XY}) behind and go on with the right hand side of the criterion which can be rewritten as:

$$\omega \quad > \quad WFR_\Omega \cdot \Omega \tag{6}$$

In this representation the right hand term can be interpreted as the circumferential gas velocity in the seal. If the gas rotates slower than the shaft (ω = precessional orbit speed) the gas brakes the shaft and therefore introduces damping. If it is faster it pushes the rotor, introduces energy into the shaft motion and therefore has a destabilizing effect. Figure 2 visualizes this interpretation.

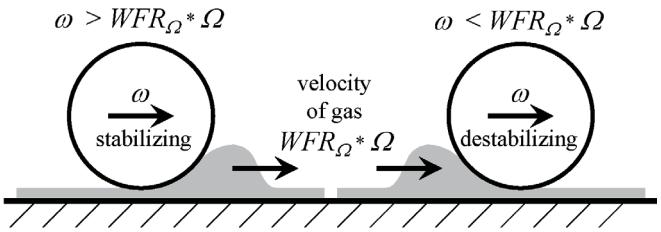

Figure 2. Simplified Representation of the Stability Criterion.

The validity of the derived stability criterion and its simplification is not only true for labyrinth seals. Also the stability behavior of cylindrical journal bearings can be predicted. In Figure 3 a typical waterfall plot of the shaft vibrations of a rotor in cylindrical bearings is shown.

As can be seen the oil whirling speed is approx. 0.4 – 0.5 which corresponds to the expected value of a "couette flow profile". According to the stability criterion the highest possible

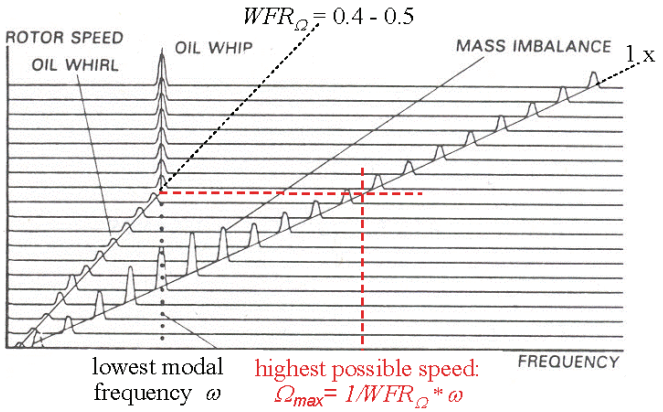

Figure 3. Waterfall Plot of a Rotor in Cylindrical Journal Bearings Showing the Typical Oil Whirl and Whip Behavior.

speed which can be reached with such a rotor is:

$$\Omega_{max} = \frac{1}{WFR_\Omega} \cdot \omega \qquad (7)$$

which is exactly where the oil whip starts and the cylindrical journal bearing becomes unstable. With labyrinth seals this threshold is not equally obvious because the forces produced in gas filled annular seal gaps are usually not as dominant and the positive damping provided by the bearings has first to be used up by the destabilizing effect of the seal.

At this point it is necessary to discuss the differences between the physically correct definition of *WFR* as the tangential force ratio and the simplified circumferential gas velocity definition. Experimental results from various investigators show a more or less linear dependency of K_{XY} of the gas swirl. Since C_{XX} is roughly independent of the gas swirl *WFR* behaves similar to K_{XY}. As can be seen in Figure 4 K_{XY} and therefore also *WFR* show negative values for zero inlet swirl.

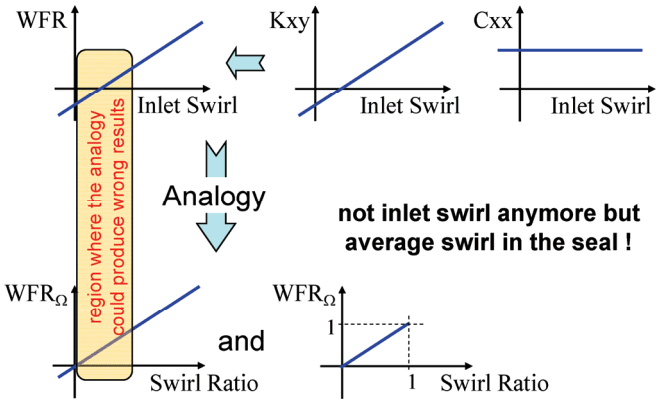

Figure 4. Visualization of the Differences Between the "Real Physics" and the Simplification.

The interpretation of WFR_Ω as circumferential gas velocity is obviously not able to reproduce this. Therefore deviations have to be expected in the low (inlet) swirl region (between zero and approx. 0.20). Since the circumferential gas velocity will always show positive values the simplification will always yield conservative results in this low (inlet) swirl region.

Another difference is that the circumferential velocity will always stay in the region between zero and one whereas the force ratio can produce negative values (as discussed above) as well as values clearly above one.

CFD ANALYSIS OF THE FLOW IN THE SEAL

Three different labyrinth types have been investigated by CFD under various conditions. The goal was to show that the developing flow pattern (and especially the circumferential velocity) is roughly independent of the operating conditions.

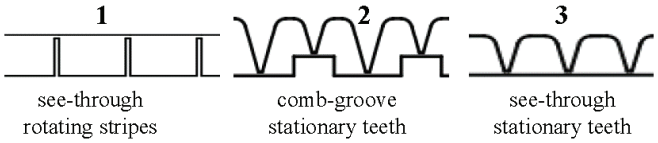

Figure 5. Investigated Labyrinth Seal Types.

These three labyrinth types were calculated with an inlet pressure of 1450 psi (100 bar) and the pressure ratio was 3. The seal length was always 25 stripes (or teeth), the inlet swirl was always zero. Additionally, with geometry No. 1 a series of calculations were carried out to investigate the influence of changing operating conditions, i.e. a pressure ratio variation (π=1.3 and π=10), a variation of the inlet pressure (435 psi and 4350 psi) as well as a calculation with an inlet swirl of 90%.

Axial Velocity

The results show that the pressure ratio has a main influence on the axial velocities. Especially for high pressure ratios the main expansion takes place in the last two cavities whereas the biggest part of the other cavities is rather unaffected by the varying pressure ratio. Figure 6 shows a contour plot of the axial velocity within the last two cavities for the variation of the pressure ratio.

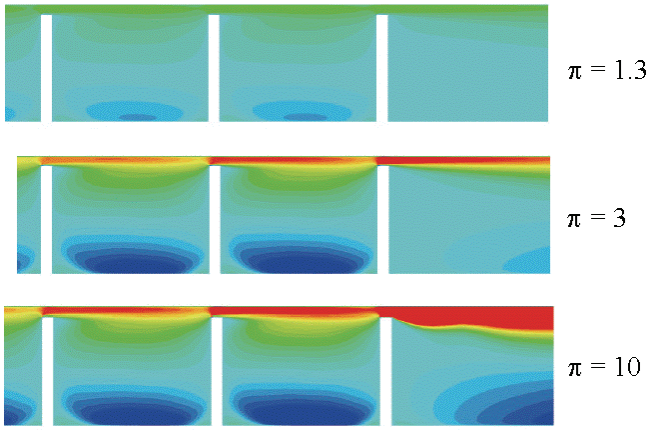

Figure 6. Axial Flow Pattern in the Last Two Cavities for Different Pressure Ratios.

Another interesting finding is that a jet stream develops in the seal gaps and that these jet stream areas are clearly separated from the cavity areas. Especially for the see-through type labyrinths only a very small amount of gas is exchanged between these areas. In the cavities a vortex is created which is driven by the boundary layer of the jet stream.

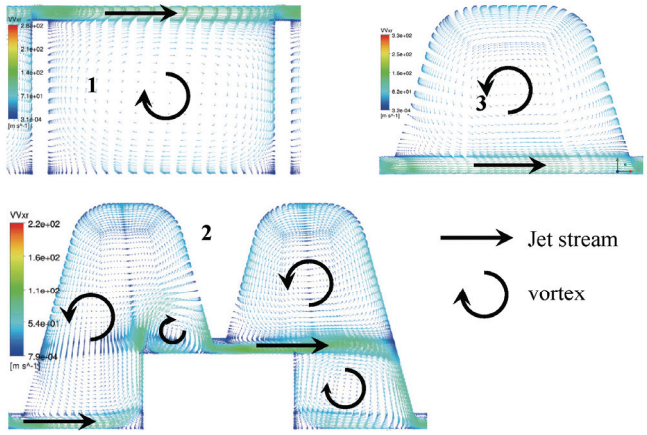

Figure 7. Vector Field of the Axial Flow Showing Distinct Jet and Vortex Regions.

Circumferential Velocity

The calculations show that the development of the circumferential flow pattern is almost not influenced by the operating conditions. Only the variation of the pressure ratio causes a slightly faster (π=1.3) or slower (π=10) build up of the circumferential velocity. As can be seen in Figure 8 this influence is minor, especially for the more realistic higher pressure ratio cases, and will therefore be neglected for the further derivation of the seal characteristics.

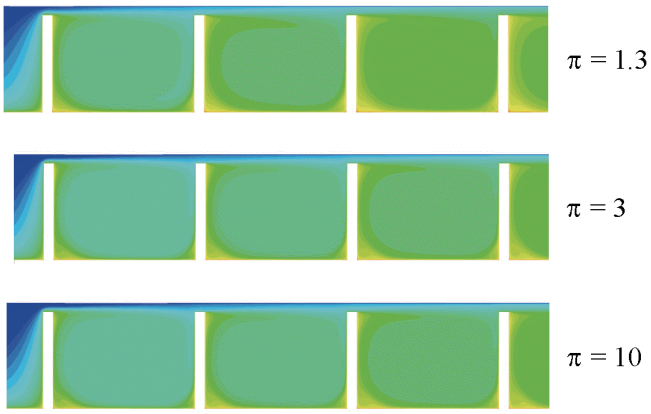

Figure 8. Circumferential Flow Pattern in the First Three Cavities for Different Pressure Ratios.

The different variation calculations show that within the degree of accuracy which can be expected of this method the varying operating conditions can be neglected and therefore only the main calculations for a medium pressure level (1450 psi inlet) and a medium pressure ratio (π=3) will be further evaluated. Figure 9 shows the most important results for the three investigated labyrinth seal types.

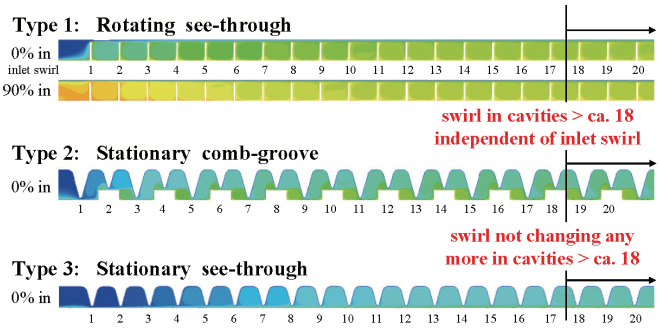

Figure 9. Pattern of the Circumferential Flow for the Three Investigated Labyrinth Types.

As can be seen each labyrinth type shows a characteristic limes for the circumferential speed of the fluid. The type and geometry of the seal defines the value of that limes. And also the speed with which this limes is reached (after how many cavities) is a function of the geometry. In order to assess correct values to the colorful plot above the circumferential speed has to be averaged in appropriate planes.

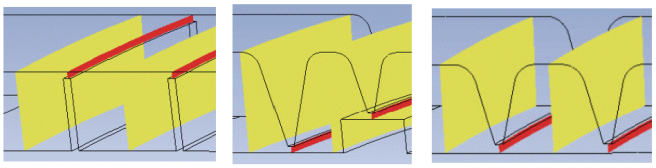

Figure 10. Averaging Planes for the Circumferential Velocity.

Since the level of the forces acting onto the rotor are always linked to the area on which those pressures and frictions are introduced, it seems adequate to place the averaging planes in the center of the cavities as shown in Figure 10 above. This averaging leads to the following analytically determined swirl diagram shown in Figure 11.

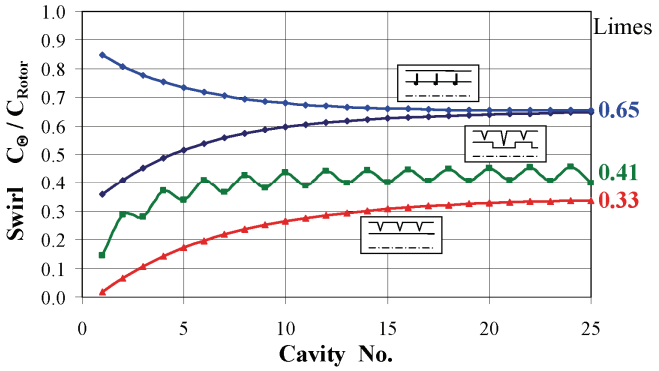

Figure 11. Analytically (CFD) Determined Averaged Swirl in the Cavities.

As can be seen in Figure 11 above the comb-groove labyrinth shows different swirls in the cavities following the long and the short teeth, respectively. Since the further calculations use the integral of the swirl (averaged in the cavities from one to n) this will later average out. The limes of

the comb-groove labyrinth as denoted above, is the average of two successive cavities.

A very interesting finding is shown in Figure 12. For the investigated geometries the analytically determined limes of the swirl is matching extremely well with the ratio between the rotating and the total cavity surfaces. If this correlation proves to be true also for other geometries (further to be investigated) this would provide an easy way to determine the swirl limes for any seal geometry without the necessity of CFD calculations.

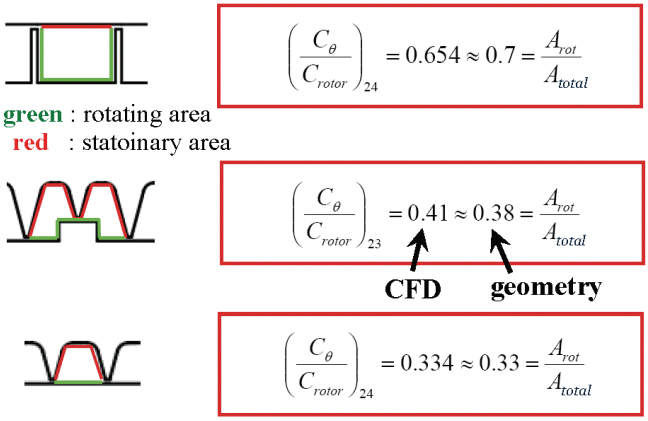

Figure 12. Correlation Between the Analytically Determined Limes of the Swirl and the Geometrical Ratio of the Rotating to the Total Cavity Area.

Curve Fitting and Averaging

In order to facilitate the calculation of the swirl for the different seal types and for arbitrary inlet conditions (swirls) it is necessary to find a single equation which fits to the CFD results. The following equation and parameters fulfill this requirement:

$$For\ I < L: \quad \frac{C_\Theta}{C_{Rotor}}(i) = L - \min\left(L - I, 0.3 \cdot \frac{L-I}{L}\right)^{1+(i-1)\cdot x} \qquad (8)$$

$$For\ I \geq L: \quad \frac{C_\Theta}{C_{Rotor}}(i) = L + \min\left(I - L, 0.3 \cdot \frac{I-L}{1-L}\right)^{1+(i-1)\cdot x} \qquad (9)$$

Where I is the inlet swirl (in the range of 0 to 1), L is the limes of the swirl for a given labyrinth type, i indicates the position in the seal (swirl in cavity No. i) and x is a factor of the exponent which controls the speed with which the swirl converges to the limes. As can be seen in Figure 9 the see-through labyrinth types build up the swirl slower than the comb-groove (or generally the stepped, true) labyrinths. With the following values for x a very good and consistent fit was achieved:

$x = 0.15$ for see-through laby types

$x = 0.35$ for comb-groove laby types

Whether the above equations and the exponent factors x are generally valid or only for the CFD calculations and configurations performed within this study, cannot be judged, but for the purpose of this tutorial it provides a good starting point with an excellent match between the parameterization and the available CFD data. Figure 13 plots the curve fits according to the equations above together with the CFD results.

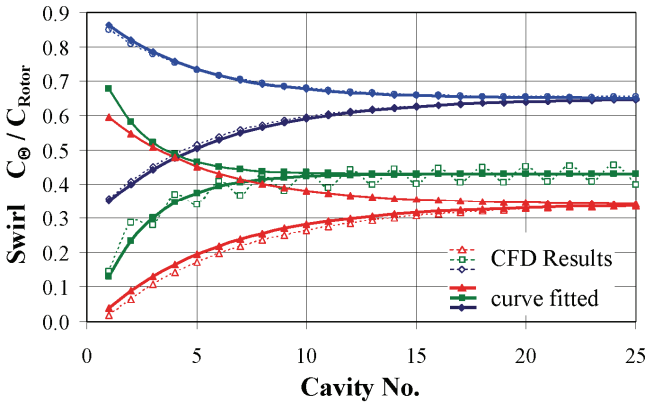

Figure 13. Plot of Original and Curve Fitted Swirl Data.

For the simplified stability calculations according to the proposed method the whirl frequency ratio WFR_Ω of a labyrinth seal is needed. Following the simplifications shown in Figure 4 WFR_Ω is the average circumferential speed of the gas in the entire seal. Thus WFR_Ω can be calculated from the Equations (8) or (9) by simply averaging the swirl values from cavity 1 to the length of the seal (n stripes or teeth).

$$WFR_\Omega = \frac{1}{n} \cdot \sum_{i=1}^{n} \frac{C_\Theta}{C_{Rotor}}(i) \qquad (10)$$

Figure 14 shows the WFR_Ω of the investigated seals and seal types according to the definitions above. Please note that the curves plotted correspond to the calculated configurations (zero and 90% inlet swirl) and again the values calculated by Equation (10) are compared to the CFD results.

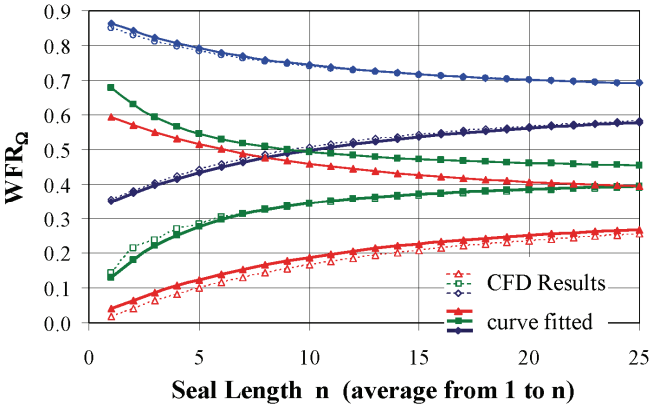

Figure 14. Plot of WFR_Ω for Different Seal Types as a Function of the Seal Length.

AVERAGE WFR_Ω OF AN ENTIRE COMPRESSOR

With the above calculations a WFR_Ω can be determined for all the seals in a compressor. In order to judge the stability behavior of a compressor it is necessary to combine the effects of these "single-seal-*WFR's*" into a "machine-*WFR*". Since the

WFR's as calculated above do not contain any information about the operating conditions of the appropriate seals, the correct weighting of the different *WFR's* is essential. In a compressor the following seals typically exist.

- impeller shroud seal
- impeller hub seal
- balance piston seal

The influence of these seals on the stability of the compressor is mainly dependent on their operating conditions but also determined by some geometrical properties. The following table gives a list of possible weighting factors:

Table 1. Possible Weighting Factors for the Determination of the WFR of an Entire Compressor.

Pressure Level	p_{in} or p_{out} or $\frac{p_{in} + p_{out}}{2}$
Pressure Difference	$p_{out} - p_{in}$
Pressure Ratio	p_{out} / p_{in}
Density	ρ_{in} or ρ_{out} or $\frac{\rho_{in} + \rho_{out}}{2}$
Seal Size	diameter and/or length (No. of stripes or teeth)
Seal Position	Position with regard to the lowest whirling modeshape

Any combination and weighting of the above factors is possible and thinkable, the list above might even be incomplete. In the course of preparing this tutorial a considerable number of such combinations have been tried. But the best results were always achieved by simply taking the pressure difference (over each seal) as the only weighting factor. And furthermore, even this very simple approach has been done in the most abstract way possible by using a linear pressure rise in the compressor:

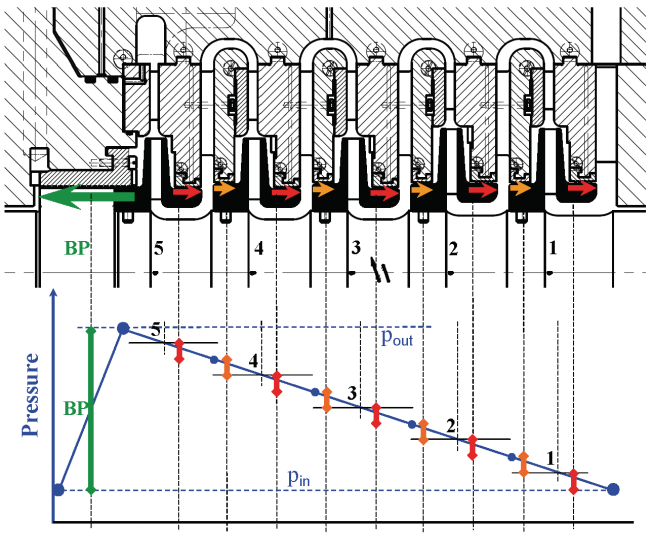

Figure 15. Schematic Representation of the Used Pressure Difference Weighting Factor.

With this further simplification no internal thermodynamic data of the compressor is needed. For the examples shown in this tutorial the only needed data is the inlet and outlet pressure (p_{in} , p_{out}) of the compressor, the number of stages (z) and an average degree of reaction (r). For other compressor designs and configurations more detailed parameters might be needed, this will have to be assessed case by case. For the calculations within this tutorial the following pressure differences over the different seal types are used:

Balance Piston: $\Delta p = p_{out} - p_{in}$

Shroud Seals: $\Delta p = (p_{out} - p_{in})/z*r$

Hub Seals: $\Delta p = (p_{out} - p_{in})/z*(1-r)$

$r = 0.5 - 0.7$

As shown in Figure 4 the biggest deviations between the proposed method and reality are expected in seals with a low preswirl because the simplified method does not produce negative values for WFR_Ω. Especially for short seals where the influence of the inlet condition is dominating the deviations can be quite significant. As can be seen in Figure 4 the proposed method will produce higher WFR_Ω values and therefore a more conservative result.

In order to minimize these deviations a valid countermeasure is to set the WFR_Ω value to zero for short seals (< 5 stripes) with zero preswirl. This should still produce conservative but much better matching results. All other seals (types, lengths, preswirls) remain unchanged and will be used as calculated by the Equations (8) and (9).

EXAMPLE CALCULATIONS

Within this tutorial two example calculations are shown. The first is a long and relatively flexible process gas compressor. For this machine the proposed method will be compared to a fully detailed level II analysis as it is required by API. In the second example the examined machine is a short and stiff high pressure compressor. With this machine extensive tests have been carried out in order to measure the damping of the rotor in loaded operation. As a side product of theses measurements the WFR_Ω value of the compressor could be experimentally determined and will now be compared to the calculation according to the proposed simplified method.

Example 1: 9-Stage Process Gas Compressor

In this first example the stability behavior of a 9-stage process gas compressor will be investigated. The comparison will be carried out by first calculating the damping of the compressor rotor without any swirl-reducing features. Step by step swirl brakes are introduced in order to determine the minimum swirl brake configuration which is needed to ensure a stabilizing seal effect (increasing damping with increasing load). Even though the damping values (*log. dec.* of the level II analysis) and the stability criterion values (WFR_Ω*FR of the simplified approach) cannot directly be compared, the change from destabilizing to stabilizing should take place at the same configuration (and therefore also at the same *WFR*).

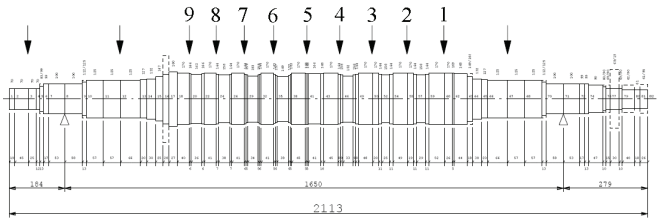

p_{in} :	3.5	bar	z :	9	-	
p_{out} :	56.3	bar	r :	0.5	-	
ρ_{in} :	3.6	kg/m³	Ω :	14‘300	rpm	FR = 3.18
ρ_{out} :	42.2	kg/m³	ω :	4‘500	rpm	

Figure 16. Process Gas Compressor Rotor and Necessary Operating Parameters.

The calculations for the API level II analysis are performed with the computer codes and modelling rules as used by the authors company for normal job applications. The calculations for the simplified approach are carried out according to the above described rules. An Excel sheet was written in order to easily vary the swirl brake configurations.

According to Figure 16 the flexi ratio of the compressor is 3.18, therefore the *WFR* for the stability threshold is 0.32. With the level II analysis this *WFR* is reached with 6 swirl brakes at the stages 4-9. With the simplified calculation 7 swirl brakes (in stages 3-9) are needed to fulfill the stability criterion. Also the comparison of the influence of the balance piston yields very similar results. Figure 17 shows a graphical representation of the comparison.

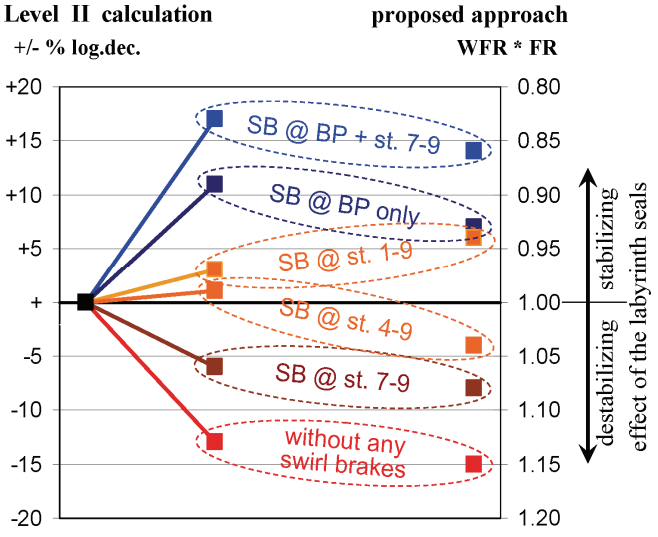

Figure 17. Comparison of the Results of the Simplified Calculation to the API Level II Analysis.

Example 2: 6-Stage High Pressure Compressor

The second example shows the high pressure compressor ULA 96. With this compressor extensive measurements have been carried out and the results were published (Baumann, 1999). Measurements of the first whirling frequency and the damping have been performed for a variety of configurations like different numbers of swirl brakes and different bearing spans. The extended bearing span was mainly introduced to lower the stability of the compressor and to facilitate better damping measurements.

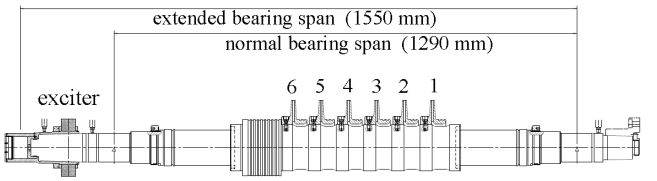

p_{in}:	180	bar	z :	6	-	
p_{out}:	450	bar	r :	0.55	-	
ρ_{in}:	120	kg/m³	Ω :	14‘141	rpm	
ρ_{out}:	260	kg/m³	ω :	6‘000	rpm (normal)	FR_{norm} = 2.36
			ω :	4‘200	rpm (extended)	FR_{ext} = 3.37

Figure 18. High Pressure Compressor Rotor Showing Two Possible Bearing Locations (normal and extended) and Operating Parameters.

Configuration ULA.5 of the mentioned publication (Baumann, 1999) was run with the extended bearing span. A swirl brake was mounted at the balance piston and three thrust brakes were installed at the stages 3, 5 and 6. The unloaded compressor exhibited a lowest natural frequency (first whirling mode) at 4200 rpm (70 Hz) which results in an unloaded flexi ratio of 3.37. The diagram in Figure 19 was obtained by running the compressor constantly at rated speed, the pressure ratio was held constant at $\pi \sim 2.5$ (staying approximately at the same location in the compressor characteristics) and the suction pressure was increased.

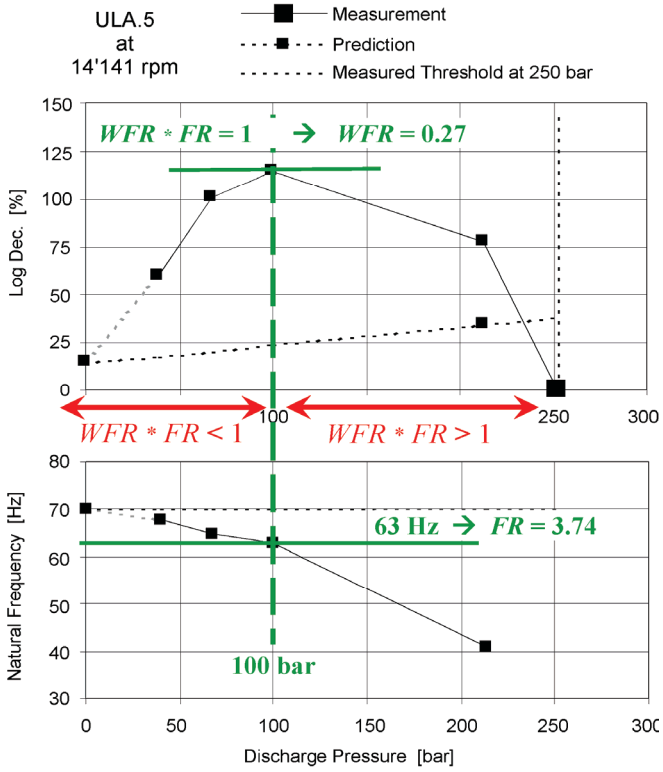

Figure 19. Measured Natural Frequency and Damping for Configuration ULA.5. (Figure 9, Baumann, 1999)

The measurements showed that with increasing load the first whirling frequency was decreasing having a negative impact on the stability as the flexi ratio increases. Assuming that the *WFR* stays approx. constant for constant operating conditions the seal effects become destabilizing at a flexi ratio of 3.74. According to Equation (5) the corresponding WFR_Ω can be determined to be 0.27.

Table 2. Calculation of the WFR According to the Simplified Approach.

Type	Stage	Location	L	x	I	n	WFR	Pr Diff	Weight
2	1	shroud	0.38	0.35	0.75	4	**0.47**	24.8	0.048
2	1	hub	0.38	0.35	0.00	4	**0.00**	20.3	0.039
2	2	shroud	0.38	0.35	0.75	4	**0.47**	24.8	0.048
2	2	hub	0.38	0.35	0.00	4	**0.00**	20.3	0.039
2	3	shroud	0.38	0.35	0.15	4	**0.29**	24.8	0.048
2	3	hub	0.38	0.35	0.00	4	**0.00**	20.3	0.039
2	4	shroud	0.38	0.35	0.75	4	**0.47**	24.8	0.048
2	4	hub	0.38	0.35	0.00	4	**0.00**	20.3	0.039
2	5	shroud	0.38	0.35	0.15	4	**0.29**	24.8	0.048
2	5	hub	0.38	0.35	0.00	4	**0.00**	20.3	0.039
2	6	shroud	0.38	0.35	0.15	4	**0.29**	24.8	0.048
2		BP	0.38	0.35	0.00	18	**0.33**	270.0	0.519
Average Whirl Frequency Ratio							WFR	**0.28**	1.000

Table 2 shows the calculation of configuration ULA.5 with the proposed simplified approach. The used preswirl of 0.75 for shroud seals having no brakes and the value of 0.15 for shroud seals having thrust brakes correspond exactly to the figures normally used for the level II analysis. Any other parameters, settings or weightings are strictly according to the procedure within this tutorial. For the weighting of the stage seals the degree of reaction of the used impellers is needed. The same impeller type is used for all six stages, for a pressure ratio of 2.5 of the entire compressor a value of 0.55 can be used for all stages. The labyrinth type is comb-groove (type 2) throughout the machine.

As can be seen in Table 2 the calculated *WFR* according to the simplified approach comes very close to the experimentally determined value.

CONCLUSION

The proposed simplified method provides a comprehensible and fast tool to judge the stability of a given rotor. The necessary input for this stability check is reduced to very few operational and geometric (design) data.

This method does not produce an absolute level of damping, therefore it is rather classifying seal effects to be stabilizing or destabilizing. Since also the basic damping of the bearings is not taken into account, the approach is rather conservative and concentrates on the seal effects only.

Despite many simplifications (in the physics as well as in the very simple swirl equations) the method produces results which are matching the calculations and observations quite accurately.

In order to generalize this method for other labyrinth geometries further CFD calculations would be necessary to confirm the validity of the very simple swirl equations.

Even though the weighting using the pressure differences only produced the best results, this judgment is based on a quite limited number of example calculations. Further investigations, especially if they consider other design features or compressor designs from other manufacturers, could lead to other weighing strategies.

Finally it has to be emphasized once again that this method does not and cannot replace a thorough level II stability analysis. But it might be a valid alternative if the quality and the details of the available data is poor and / or if no high sophisticated rotordynamic tools are available.

NOMENCLATURE

A_{rot}	= rotating cavity surface area	[m^2]
A_{total}	= entire cavity surface area (rot & stat)	[m^2]
C_{XX}	= direct damping	[Ns / m]
C_{eff}	= effective damping of the seal	[Ns / m]
C_{Rotor}	= circumferential speed of the rotor	[m / s]
C_Θ	= circumferential speed of the gas	[m / s]
FR	= flexi ratio	[-]
F_Θ	= tangential seal force	[N]
I	= relative inlet swirl of the gas	[-]
K_{XY}	= cross-coupling stiffness	[N / m]
L	= limes of the relative circumf. speed	[-]
N	= rotor speed	[rpm]
n	= length of the laby (stripes or teeth)	[-]
p_{in}	= compressor inlet pressure	[bar]
p_{out}	= compressor outlet pressure	[bar]
r	= degree of reaction	[-]
r_0	= orbit radius	[m]
WFR	= whirl frequency ratio	[-]
WFR_Ω	= WFR based on the shaft speed	[-]
WFR_ω	= WFR based on the lowest mode	[-]
x	= swirl convergence exponent	[-]
z	= number of stages of the compressor	[-]
Δp	= pressure difference	[bar]
π	= pressure ratio	[-]
ρ_{in}	= compressor inlet density	[kg / m^3]
ρ_{out}	= compressor outlet density	[kg / m^3]
Ω	= angular speed of the shaft	[1 / s]
ω	= angular speed of the lowest mode	[1 / s]

REFERENCES

Baumann, U., 1999, "Rotordynamic Stability Tests on High-Pressure Radial Compressors," Proceedings of the 28th Turbomachinery Symposium, Turbomachinery Laboratory, Texas A&M University, College Station, Texas, pp. 115-122.